Reactivity of Hydrides $FeH_2(CO)_2P_2$ (P = Phosphites) with Aryldiazonium Cations: Preparation, Characterization, X-ray Crystal Structure, and Electrochemical Studies of Mono- and Binuclear Aryldiazenido Complexes

Gabriele Albertin,*,† Stefano Antoniutti,† Alessia Bacchi,‡ Davide Barbera,† Emilio Bordignon,† Giancarlo Pelizzi,‡ and Paolo Ugo§

Dipartimento di Chimica and Dipartimento di Chimica Fisica, Università Ca' Foscari di Venezia, Dorsoduro 2137, 30123 Venezia, Italy, and Dipartimento di Chimica Generale ed Inorganica, Chimica Analitica, Chimica Fisica, Centro CNR di Strutturistica Diffrattometrica, Università di Parma, Viale delle Scienze, 43100 Parma, Italy

Received April 16, 1998

Mono- and binuclear aryldiazenido complexes $[Fe(ArN_2)(CO)_2P_2]BPh_4$ (**1**−**4**) and $[\{Fe(CO)_2P_2\}_2(\mu\text{-}N_2Ar{-}ArN_2)](BPh_4)_2$ (**5**−**8**) [P = $P(OEt)_3$, $PPh(OEt)_2$, PPh_2OEt, $P(OPh)_3$; Ar = C_6H_5, 2-$CH_3C_6H_4$, 4-$CH_3C_6H_4$; Ar−Ar = 4,4′-$C_6H_4{-}C_6H_4$, 4,4′-(2-CH_3)$C_6H_3{-}C_6H_3$(2-CH_3), 4,4′-$C_6H_4{-}CH_2{-}C_6H_4$] were prepared by allowing hydride species $FeH_2(CO)_2P_2$ to react with an excess of mono- $(ArN_2)(BF_4)$ or bis-aryldiazonium $(N_2Ar{-}ArN_2)(BF_4)_2$ salts, respectively, at low temperature. A reaction path involving a hydride−aryldiazene intermediate $[FeH(ArN{=}NH)(CO)_2P_2]^+$, which, through the loss of H_2, affords the final aryldiazenido complexes **1**−**8**, is proposed. The compounds were characterized by ^1H and $^{31}P\{^1H\}$ NMR spectroscopy (including ^{15}N isotopic substitution) and X-ray crystal structure determination. The complex $[Fe(CO)_2\{P(OEt)_3\}_2\{\mu\text{-}4,4'\text{-}N_2(2\text{-}CH_3)C_6H_3{-}C_6H_3(2\text{-}CH_3)N_2\}](BPh_4)_2$ (**5b**) crystallizes in the space group $P\bar{1}$ with $a = 15.008(4)$ Å, $b = 17.094(5)$ Å, $c = 10.553(3)$ Å, $\alpha = 99.56(1)°$, $\beta = 102.80(1)°$, $\gamma = 65.30(1)°$, and $Z = 1$. The structure is centrosymmetric and consists of binuclear cations with the two iron atoms in a quite regular trigonal bipyramidal environment, with the two CO in the equatorial and the two phosphites in the apical position, respectively. Aryldiazenido complexes **1**−**8** react with strong acids HX (X = Cl, CF_3SO_3, CF_3CO_2) to give the corresponding aryldiazene derivatives, according to the equilibrium $[Fe(ArN_2)(CO)_2P_2]^+ + HX \rightleftharpoons [FeX(ArN{=}NH)(CO)_2P_2]^+$. Electrochemical studies of both mono- (**1**−**4**) and binuclear (**5**−**8**) compounds were undertaken, and a mechanism for oxidation and reduction processes is proposed.

Introduction

Previous reports[1−5] from our laboratory have dealt with studies on the reactions of metal(II) dihydrides MH_2P_4 (M = Fe, Ru, Os; P = phosphite) with aryldiazonium cations, which proceed to give mono- and bis(aryldiazene) $[MH(ArN{=}NH)P_4]BPh_4$ and $[M(ArN{=}NH)_2P_4](BPh_4)_2$ derivatives through the insertion of the ArN_2^+ cations into the M−H bonds. We have now extended these studies to include the reactivity of iron dihydrides $FeH_2(CO)_2P_2$ with aryldiazonium cations and found, instead of aryldiazene complexes, the formation of aryldiazenido $[Fe(ArN_2)(CO)_2P_2]^+$ cations in good yields.

In view of current interest[6−29] in the chemistry of the "diazo" complexes, due not only to their relevance to the nitrogen fixation process but also to their diverse reactivity modes and structural properties, this paper reports the synthesis and

† Dipartimento di Chimica, Università Ca' Foscari di Venezia.
‡ Dipartimento di Chimica Generale ed Inorganica, Università di Parma.
§ Dipartimento di Chimica Fisica, Università Ca' Foscari di Venezia.

(1) Albertin, G.; Antoniutti, S.; Pelizzi, G.; Vitali, F.; Bordignon, E. *J. Am. Chem. Soc.* **1986**, *108*, 6627.
(2) Albertin, G.; Antoniutti, S.; Bordignon, E. *Inorg. Chem.* **1987**, *26*, 3416.
(3) Albertin, G.; Antoniutti, S.; Pelizzi, G.; Vitali, F.; Bordignon, E. *Inorg. Chem.* **1988**, *27*, 829.
(4) Albertin, G.; Antoniutti, S.; Bordignon, E. *J. Chem. Soc., Dalton Trans.* **1989**, 2353.
(5) Albertin, G.; Antoniutti, S.; Bacchi, A.; Bordignon, E.; Pelizzi, G.; Ugo, P. *Inorg. Chem.* **1996**, *35*, 6245.
(6) Zollinger, H. *Diazo Chemistry II*; VCH: Weinheim, Germany, 1995.
(7) Sutton, D. *Chem. Rev.* **1993**, *93*, 995.
(8) Kisch, H.; Holzmeier, P. *Adv. Organomet. Chem.* **1992**, *34*, 67.
(9) Johnson, B. F. G.; Haymore, B. L.; Dilworth, J. R. In *Comprehensive Coordination Chemistry*; Wilkinson, G., Gillard, R. D., McCleverty, J. A., Eds.; Pergamon Press: Oxford, U.K., 1987; Vol. 2, p 130.
(10) Henderson, R. A.; Leigh, G. J.; Pickett, C. J. *Adv. Inorg. Chem. Radiochem.* **1983**, *27*, 197.
(11) Nugent, W. A.; Haymore, B. L.; *Coord. Chem. Rev.* **1980**, *31*, 123.
(12) Bottomley, F. *Quart. Rev.* **1970**, *24*, 617.
(13) Hidai, M.; Mizobe, Y. *Chem. Rev.* **1995**, *95*, 1115.
(14) Eady, R. R.; Leigh, G. J. *J. Chem. Soc., Dalton Trans.* **1994**, 2739.
(15) Sellmann, D. *Angew. Chem., Int. Ed. Engl.* **1993**, *32*, 64.
(16) Yan, X.; Batchelor, R. J.; Einstein, F. W. B.; Zhang, X.; Nagelkerke, R.; Sutton, D. *Inorg. Chem.* **1997**, *36*, 1237.
(17) Lehnert, N.; Wiesler, B. E.; Tuczek, F.; Hennige, A.; Sellmann, D. *J. Am. Chem. Soc.* **1997**, *36*, 8869.
(18) Hirsch-Kuchma, M.; Nicholson, T.; Davison, A.; Davis, W. M.; Jones, A. G. *Inorg. Chem.* **1997**, *36*, 3237.
(19) Garcia-Minsal, A.; Sutton, D. *Organometallics* **1996**, *15*, 332.
(20) Rose, D. J.; Maresca, K. P.; Kettler, P. B.; Chang, Y. D.; Saghomomian, V.; Chen, Q.; Abrams, M. J.; Larsen, S. K.; Zubieta, J. *Inorg. Chem.* **1996**, *35*, 3548.
(21) Cusanelli, A.; Sutton, D. *Organometallics* **1995**, *14*, 4651.
(22) Kettler, P. B.; Chang, Y.-D.; Zubieta, J. *Inorg. Chem.* **1994**, *33*, 5864.
(23) Kim, G. C.-Y.; Batchelor, R. J.; Yan, X.; Einstein, F. W. B.; Sutton, D. *Inorg. Chem.* **1995**, *34*, 6163.
(24) Demadis, K. D.; Malinak, S. M.; Coucouvanis, D. *Inorg. Chem.* **1996**, *35*, 4038.
(25) Cheng, T.-Y.; Ponce, A.; Rheingold, A. L.; Hillhouse, G. L. *Angew. Chem., Int. Ed. Engl.* **1994**, *33*, 657.
(26) Sellmann, D.; Käppler, J.; Moll, M.; Knoch, F. *Inorg. Chem.* **1993**, *32*, 960.

10.1021/ic980430e CCC: $15.00
Published on Web 10/02/1998

Chart 1

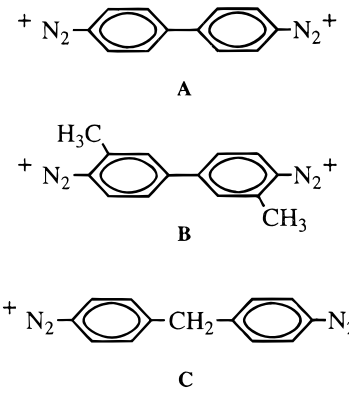

characterization of new aryldiazenido complexes of iron, together with detailed studies on the reaction course between $FeH_2(CO)_2P_2$ and ArN_2^+. The use of bis(aryldiazonium) cations $(N_2Ar-ArN_2)(BF_4)_2$ as reagents (Chart 1) also yields binuclear complexes with a bis(diazenido) bridging ligand whose first X-ray crystal structure determination is also reported here, together with an electrochemical study of the new aryldiazenido derivatives.

Experimental Section

All synthetic work was carried out in appropriate atmospheres (Ar, N_2) using standard Schlenk techniques or a Vacuum Atmosphere drybox. All solvents were dried over appropriate drying agents, degassed on a vacuum line, and distilled into vacuum-tight storage flasks. Triethyl phosphite and triphenyl phosphite were Aldrich products; phosphines $PPh(OEt)_2$ and PPh_2OEt were prepared by the method of Rabinowitz and Pellon.[30] Diazonium salts were obtained in the usual way.[31] Related bis(diazonium) $[N_2Ar-ArN_2](BF_4)_2$ [Ar−Ar = 4,4′-$C_6H_4-C_6H_4$, **A**; 4,4′-(2-CH_3)$C_6H_3-C_6H_3$(2-CH_3), **B**; 4,4′-$C_6H_4-CH_2-C_6H_4$, **C**] salts were prepared by treating the amine precursors $H_2NAr-ArNH_2$ with $NaNO_2$, as described in the literature for the common mono(diazonium) salts.[31] Labeled diazonium tetrafluoroborates $[C_6H_5N{\equiv}{}^{15}N]BF_4$ and $[4,4'\text{-}{}^{15}N{\equiv}NC_6H_4-C_6H_4N{\equiv}{}^{15}N](BF_4)_2$ were prepared from $Na^{15}NO_2$ (99% enriched, CIL) and the appropriate amine. *p*-Tolyl isocyanide was obtained by the phosgene method of Ugi et al.[32] Other reagents were purchased from commercial sources in the highest available purity and used as received. Infrared spectra were recorded on Digilab Bio-Rad FTS-40 or Nicolet Magna 750 FT-IR spectrophotometers. NMR spectra (^1H, ^{13}C, ^{31}P, ^{15}N) were obtained on a Bruker AC200 spectrometer at temperatures varying between +30 and −90 °C, unless otherwise noted. ^1H and ^{13}C spectra refer to internal tetramethylsilane. $^{31}P\{^1H\}$ chemical shifts are reported with respect to 85% H_3PO_4, with downfield shifts considered positive. ^{15}N spectra refer to external $CH_3{}^{15}NO_2$, with downfield shifts considered positive. The SwaN-MR software package[33] has been used in treating the NMR data. All spectroscopic data are summerized in Table 1. The conductivities of 10^{-3} M solutions of the complexes in CH_3NO_2 at 25 °C were measured with a Radiometer CDM 83 instrument.

Synthesis of Complexes. Hydrides $FeH_2(CO)_2[P(OEt)_3]_2$ and $FeH_2(CO)_2[P(OPh)_3]_2$ were prepared as previously reported.[34]

a. $FeH_2(CO)_2P_2$ [P = $PPh(OEt)_2$ and PPh_2OEt]. These complexes were prepared by reacting $K[FeH(CO)_4]$ with the appropriate phosphite following the method reported for the related $P(OEt)_3$ and $P(OPh)_3$ derivatives.[34] A reaction time of 5 h was used, and the complexes were extracted with a mixture of petroleum ether (40−60 °C) and benzene (4:1 ratio) giving, after crystallization, a light-green oil at room temperature; yield ≥ 85%. For P = $PPh(OEt)_2$: IR, 1998, 1954 [s, ν(CO)] cm^{-1}; ^1H NMR ($CD_3C_6D_5$, 25 °C), δ 7.56−6.90 (m, 10 H, Ph), 3.64, 3.44 (m, 8 H, CH_2), 0.84 (t, 12 H, CH_3), −10.40 (t, 2 H, hydride); $^{31}P\{^1H\}$ NMR ($CD_3C_6D_5$, 25 °C), δ 196.0 (s). For P = PPh_2OEt: IR, 1991, 1952 [s, ν(CO)] cm^{-1}; ^1H NMR ($CD_3C_6D_5$, 25 °C), δ 7.60−6.70 (m, 20 H, Ph), 3.50 (m, 4 H, CH_2), 0.82 (t, 6 H, CH_3), −9.83 (t, 2 H, hydride); $^{31}P\{^1H\}$ NMR ($CD_3C_6D_5$, 25 °C), δ 171.6 (s).

b. $[Fe(ArN_2)(CO)_2P_2]BPh_4$ (1−4) [P = $P(OEt)_3$ (1), $PPh(OEt)_2$ (2), PPh_2OEt (3), $P(OPh)_3$ (4); Ar = C_6H_5 (a), 2-$CH_3C_6H_4$ (b), 4-$CH_3C_6H_4$ (c)]. A solution of the appropriate hydride $FeH_2(CO)_2P_2$ (2 mmol) in 15 mL of CH_2Cl_2 was cooled to −80 °C and quickly transferred by needle into a reaction flask containing an excess of the aryldiazonium salt (5 mmol), previously cooled to −80 °C. The reaction mixture was allowed to reach room temperature, stirred for 7−8 h, and then filtered to remove the unreacted diazonium salt. The solvent was removed under reduced pressure, giving a brown oil, which was treated with 5 mL of ethanol. The addition of an excess of $NaBPh_4$ (4 mmol, 1.37 g) in 5 mL of ethanol to the resulting solution caused the precipitation of a red solid, which was filtered and crystallized from CH_2Cl_2 (3 mL) and ethanol (5 mL). In some cases, mainly with $PPh(OEt)_2$ or PPh_2OEt derivatives (**2c**, **3c**), an oil was obtained after the addition of $NaBPh_4$ that was dissolved in acetone and chromatographed through a silica gel column (20 cm × 2 cm) using acetone as eluent. The eluate (60 mL) was evaporated to dryness, giving an oil, which was triturated with 4 mL of ethanol. After the mixture was stirred for 2−3 h, a red solid separated out from the solution, which was filtered and dried under vacuum; yield from 40 to 70%. Anal. Calcd for **1a**: C, 60.85; H, 6.38; N, 3.23. Found: C, 61.01; H, 6.40; N, 3.40. Λ_M = 49.3 Ω^{-1} mol^{-1} cm^2. Anal. Calcd for **1b**: C, 61.24; H, 6.51; N, 3.17. Found: C, 61.07; H, 6.42; N, 3.10. Λ_M = 51.6 Ω^{-1} mol^{-1} cm^2. Anal. Calcd for **1c**: C, 61.24; H, 6.51; N, 3.17. Found: C, 61.35; H, 6.30; N, 3.08. Λ_M = 57.8 Ω^{-1} mol^{-1} cm^2. Anal. Calcd for **2c**: C, 67.25; H, 6.07; N, 2.96. Found: C, 67.02; H, 6.20; N, 3.01. Λ_M = 58.2 Ω^{-1} mol^{-1} cm^2. Anal. Calcd for **3c**: C, 72.49; H, 5.86; N, 2.77. Found: C, 72.65; H, 5.78; N, 2.64. Λ_M = 54.8 Ω^{-1} mol^{-1} cm^2. Anal. Calcd for **4b**: C, 70.78; H, 4.91; N, 2.39. Found: C, 70.65; H, 4.83; N, 2.31. Λ_M = 53.6 Ω^{-1} mol^{-1} cm^2. Anal. Calcd for **4c**: C, 70.78; H, 4.91; N, 2.39. Found: C, 70.65; H, 4.77; N, 2.35. Λ_M = 52.9 Ω^{-1} mol^{-1} cm^2.

c. $[Fe(C_6H_5N{\equiv}{}^{15}N)(CO)_2\{P(OEt)_3\}_4]BPh_4$ (1a$_1$). This compound was prepared exactly like the related compound **1a** using the labeled $[C_6H_5N{\equiv}{}^{15}N]^+BF_4^-$ aryldiazonium salt; yield ≥ 60%.

d. $[\{Fe(CO)_2P_2\}_2(\mu\text{-}N_2Ar-ArN_2)](BPh_4)_2$ (5−8) [P = $P(OEt)_3$ (5), $PPh(OEt)_2$ (6), PPh_2OEt (7), $P(OPh)_3$ (8); Ar−Ar = 4,4′-$C_6H_4-C_6H_4$ (a), 4,4′-(2-CH_3)$C_6H_3-C_6H_3$(2-CH_3) (b), 4,4′-$C_6H_4-CH_2-C_6H_4$ (d)]. A solution of the appropriate hydride $FeH_2(CO)_2P_2$ (2 mmol) in 30 mL of acetone was cooled to about −80 °C and quickly transferred by needle into a 50 mL three-necked round-bottomed flask cooled to −80 °C and containing an excess of the bis(aryldiazonium) salt (3 mmol). The reaction mixture was brought to room temperature, stirred for about 12 h, and then filtered to separate the unreacted diazonium salt. The resulting solution was evaporated to dryness under reduced pressure, giving a red-brown oil, which was treated with 5 mL of ethanol. The addition of an excess of $NaBPh_4$ (4 mmol, 1.37 g) in 5 mL of ethanol caused the separation of a red solid in some cases and of a red oil in others (**6a**, **7a**, **7b**). All the compounds, however, were purified by chromatography on silica gel using a 30 cm × 2 cm column and acetone as an eluent. The first eluate (about 80 mL) was evaporated to dryness under reduced pressure, giving an oil, which was triturated with 5 mL of ethanol. A red solid slowly separated out under vigorous stirring, which was filtered and dried under vacuum; yield from 40 to

(27) Glassman, T. E.; Vale, M. G.; Schrock, R. R. *J. Am. Chem. Soc.* **1992**, *114*, 8098.
(28) Kawano, M.; Hoshino, C.; Matsumoto, K. *Inorg. Chem.* **1992**, *31*, 5158.
(29) Vogel, S.; Barth, A.; Huttner, G.; Klein, T.; Zsolnai, L.; Kremer, R. *Angew. Chem., Int. Ed. Engl.* **1991**, *30*, 303.
(30) Rabinowitz, R.; Pellon, J. *J. Org. Chem.* **1961**, *26*, 4623.
(31) Vogel, A. I. *Practical Organic Chemistry*, 3rd ed.; Longmans, Green and Co.: New York, 1956.
(32) Ugi, I.; Fetzer, U.; Eholzer, W.; Knupfer, H.; Offermann, K. *Angew. Chem., Int. Ed. Engl.* **1965**, *4*, 472.
(33) Balacco, G. *J. Chem. Inf. Comput. Sci.* **1994**, *34*, 1235.
(34) Brunet, J. J.; Kindela, F. B.; Neibecker, D. *Inorg. Synth.* **1992**, *29*, 156.

Table 1. Selected IR and NMR Data for Iron Complexes

	IR[b]		^{1}H NMR[c,d]		^{31}P{^{1}H} NMR[c,e]
compd[a]	ν, cm^{-1}	assgnt	δ	assgnt	δ
1a $[Fe(C_6H_5N_2)(CO)_2\{P(OEt)_3\}_2]^+$	2045, s	ν_{CO}	4.27, m	CH_2	145.8, s
	1988, s		1.29, t	CH_3	
	1743, m	ν_{N_2}			
1a$_1$ $[Fe(C_6H_5N{\equiv}{}^{15}N)(CO)_2\{P(OEt)_3\}_2]^+$	2044, s	ν_{CO}	4.27, m	CH_2	145.8, d
	1988, s		1.28, t	CH_3	$^2J_{^{15}NP} = 20$ Hz
	1708, m	$\nu^{15}_{N{\equiv}N}$			
1b $[Fe(2\text{-}CH_3C_6H_4N_2)(CO)_2\{P(OEt)_3\}_2]^+$	2040, s	ν_{CO}	4.26, m	CH_2	146.5, s
	1977, s		2.35, s	CH_3	
	1751, m	ν_{N_2}	1.29, t	CH_3 phos	
1c $[Fe(4\text{-}CH_3C_6H_4N_2)(CO)_2\{P(OEt)_3\}_2]^+$	2040, s	ν_{CO}	4.26, m	CH_2	146.3, s
	1984, s		2.43, s	CH_3	
	1736, m	ν_{N_2}	1.29, t	CH_3 phos	
2c $[Fe(4\text{-}CH_3C_6H_4N_2)(CO)_2\{PPh(OEt)_2\}_2]^+$	2033, s	ν_{CO}	4.23, m	CH_2	173.0, s
	1978, s		2.35, s	CH_3	
	1734, m	ν_{N_2}	1.35, t	CH_3 phos	
3c $[Fe(4\text{-}CH_3C_6H_4N_2(CO)_2(PPh_2OEt)_2]^+$	2028, s	ν_{CO}	4.05, m	CH_2	152.8, s
	1972, s		3.57, m		
	1731, m	ν_{N_2}	2.32, s	CH_3	
			1.29, t	CH_3 phos	
			1,12, t		
4b $[Fe(2\text{-}CH_3C_6H_4N_2)(CO)_2\{P(OPh)_3\}_2]^+$	2056, s	ν_{CO}	2.19, s	CH_3	147.0, s
	1992, s				
	1779, m	ν_{N_2}			
4c $[Fe(4\text{-}CH_3C_6H_4N_2)(CO)_2\{P(OPh)_3\}_2]^+$	2055, s	ν_{CO}	2.46, s	CH_3	146.7, s
	1987, s				
	1776, m	ν_{N_2}			
5a $\{[Fe(CO)_2\{P(OEt)_3\}_2]_2(\mu\text{-}4,4'\text{-}N_2C_6H_4{-}C_6H_4N_2)\}^{2+}$	2046, s	ν_{CO}	4.30, m	CH_2	145.4, s
	1991, s		1.30, t	CH_3	(147.6, s)[f]
	1733, m	ν_{N_2}			
5a$_1$ $\{[Fe(CO)_2\{P(OEt)_3\}_2]_2(\mu\text{-}4,4'\text{-}{}^{15}N{\equiv}NC_6H_4{-}C_6H_4N{\equiv}{}^{15}N)\}^{2+}$ [g]	2040, s	ν_{CO}	4.30, m	CH_2	145.4, d
	1992, s		1.31, t	CH_3	$^2J_{^{15}NP} = 20$ Hz
	1701, m	$\nu^{15}_{N{\equiv}N}$			
5b $\{[Fe(CO)_2\{P(OEt)_3\}_2]_2[\mu\text{-}4,4'\text{-}N_2(2\text{-}CH_3)C_6H_3{-}C_6H_3(2\text{-}CH_3)N_2]\}^{2+}$	2042, s	ν_{CO}	4.27, m	CH_2	146.0, s
	1987, s		2.39, s	CH_3	
	1743, m	ν_{N_2}	1.30, t	CH_3 phos	
5d $\{[Fe(CO)_2\{P(OEt)_3\}_2]_2(\mu\text{-}4,4'\text{-}N_2C_6H_4{-}CH_2{-}C_6H_4N_2)\}^{2+}$	2042, s	ν_{CO}	4.26, m	CH_2 phos	146.0, s
	1988, s		4.18, s	CH_2 diazo	
	1735, m	ν_{N_2}	1.27, t	CH_3	
6a $\{[Fe(CO)_2\{PPh(OEt)_2\}_2]_2(\mu\text{-}4,4'\text{-}N_2C_6H_4{-}C_6H_4N_2)\}^{2+}$	2036, s	ν_{CO}	4.25, br	CH_2	170.0, s
	1982, s		1.35, t	CH_3	
	1720, m	ν_{N_2}			
6b $\{[Fe(CO)_2\{PPh(OEt)_2\}_2]_2[\mu\text{-}4,4'\text{-}N_2(2\text{-}CH_3)C_6H_3{-}C_6H_3(2\text{-}CH_3)N_2]\}^{2+}$	2035, s	ν_{CO}	4.28, m	CH_2	170.6, s
	1980, s		2.27, s	CH_3	
	1733, m	ν_{N_2}	1.39, t	CH_3 phos	
7a $[\{Fe(CO)_2(PPh_2OEt)_2\}_2(\mu\text{-}4,4'\text{-}N_2C_6H_4{-}C_6H_4N_2)]^{2+}$	2030, s	ν_{CO}	4.10, m	CH_2	152.4, s
	1973, s		3.57, m		
	1723, m	ν_{N_2}	1.33, t	CH_3	
			1.13, t		
7b $[\{Fe(CO)_2(PPh_2OEt)_2\}_2\{\mu\text{-}4,4'\text{-}N_2(2\text{-}CH_3)C_6H_3{-}C_6H_3(2\text{-}CH_3)N_2\}]^{2+}$	2028, s	ν_{CO}	4.08, m	CH_2	153.1, s
	1972, s		3.58, m		
	1733, m	ν_{N_2}	2.40, s	CH_3	
			1.31, t	CH_3 phos	
			1,13, t		
8a $\{[Fe(CO)_2\{P(OPh)_3\}_2]_2(\mu\text{-}4,4'\text{-}N_2C_6H_4{-}C_6H_4N_2)\}^{2+}$	2054, s	ν_{CO}			149.2, s[f]
	2000, s				
	1759, m	ν_{N_2}			

[a] All compounds are BPh_4^- salts. [b] In KBr pellets. [c] At room temperature in $(CD_3)_2CO$, unless otherwise noted. [d] Phenyl proton resonances are omitted. [e] Positive shift downfield from 85% H_3PO_4. [f] At −80 °C. [g] ^{15}N NMR (CD_2Cl_2, 25 °C): δ 19.7 t ($^2J_{^{15}N^{31}P} = 20$ Hz).

70%. Anal. Calcd for **5a**: C, 60.92; H, 6.27; N, 3.23. Found: C, 60.75; H, 6.31; N, 3.16. $\Lambda_M = 123\ \Omega^{-1}\ mol^{-1}\ cm^2$. Anal. Calcd for **5b**: C, 61.31; H, 6.40; N, 3.18. Found: C, 61.46; H, 6.47; N, 3.16. $\Lambda_M = 112\ \Omega^{-1}\ mol^{-1}\ cm^2$. Anal. Calcd for **5d**: C, 61.12; H, 6.34; N, 3.20. Found: C, 61.25; H, 6.21; N, 3.08. $\Lambda_M = 118\ \Omega^{-1}\ mol^{-1}\ cm^2$. Anal. Calcd for **6a**: C, 67.04; H, 5.84; N, 3.01. Found: C, 67.16; H, 6.02; N, 2.93. $\Lambda_M = 124\ \Omega^{-1}\ mol^{-1}\ cm^2$. Anal. Calcd for **6b**: C, 67.32; H, 5.97; N, 2.96. Found: C, 67.19; H, 6.10; N, 2.88. $\Lambda_M = 123\ \Omega^{-1}\ mol^{-1}\ cm^2$. Anal. Calcd for **7a**: C, 72.38; H, 5.47; N, 2.81. Found: C, 72.21; H, 5.41; N, 2.75. $\Lambda_M = 136\ \Omega^{-1}\ mol^{-1}\ cm^2$. Anal. Calcd for **7b**: C, 72.56; H, 5.59; N, 2.77. Found: C, 72.39; H, 5.50; N, 2.66. $\Lambda_M = 129\ \Omega^{-1}\ mol^{-1}\ cm^2$. Anal. Calcd for **8a**: C, 70.67; H, 4.71; N, 2.42. Found: C, 70.54; H, 4.63; N, 2.37. $\Lambda_M = 125\ \Omega^{-1}\ mol^{-1}\ cm^2$.

e. $[\{Fe(CO)_2[P(OEt)_3]_2\}_2(\mu\text{-}4,4'\text{-}{}^{15}N{\equiv}NC_6H_4{-}C_6H_4N{\equiv}{}^{15}N)](BPh_4)_2$ (5a$_1$). This compound was prepared like the related **5a** using the labeled $[4,4'\text{-}{}^{15}N{\equiv}NC_6H_4{-}C_6H_4N{\equiv}{}^{15}N](BF_4)_2$ bis(diazonium) salt; yield ≥ 70%.

Protonation Reactions. The protonation reactions of aryldiazenido complexes **1a**, **1a$_1$**, **1c**, and **5a** were carried out both in a 25 mL three-necked round-bottomed flask and in a 5-mm NMR tube. In all cases, an excess of the appropriate acid (CF_3SO_3H, CF_3COOH, or HCl 0.1 M in diethyl ether) was added to the solution of the complex cooled to −80 °C and, after room temperature was reached, the progress of the

Table 2. X-ray Diffraction Data Collection and Structure Refinement for Compound $[\{Fe(CO)_2[P(OEt)_3]_2\}_2\text{-}\{\mu\text{-}4,4'\text{-}N_2(2\text{-}CH_3)C_6H_3{-}C_6H_3(2\text{-}CH_3)N_2\}](BPh_4)_2$ (**5b**)

chem formula: $C_{90}H_{112}B_2Fe_2N_4O_{16}P_4$	$\mu = 0.43$ mm^{-1}
fw = 1763.04	$F(000) = 930$
crystal system: triclinic	absorption $T_{max}/T_{min} = 1.11/0.83$
space group: $P\bar{1}$	scan mode = $\theta-2\theta$
radiation: Mo Kα	θ range = 3−28°
$\lambda = 0.710\ 69$ Å	index range = $-19 \le h \le 19$, $-22 \le k \le 22$, $0 \le l \le 13$
$a = 15.008(4)$ Å	
$b = 17.094(5)$ Å	measured reflections = 11 524
$c = 10.553(3)$ Å	independent reflections = 11 524
$\alpha = 99.56(1)°$	observed reflections [$I \ge 2\sigma(I)$] = 3117
$\beta = 102.80(1)°$	parameters/restraints = 492/234
$\gamma = 65.30(1)°$	$\Delta\rho_{max,min} = 0.41/-0.36$ e Å^{-1}
$V = 2390(1)$ Å^3	R1[a] (observed data) = 0.0717
$Z = 1$	wR2[b] (all data) = 0.3003
$D_{calcd} = 1.22$ g cm^{-3}	goodness of fit = 0.875

[a] $R1 = \sum||F_o| - |F_c||/\sum|F_o|$. [b] $wR2 = \{\sum[w(F_o^2 - F_c^2)^2]/\sum[w(F_o^2)^2]\}^{1/2}$; $w = 1/[\sigma^2(F_o^2) + (aP)^2 + bP]$, $P = [2F_c^2 + \max(F_o^2,0)]/3$.

reaction was monitored by both IR (using 0.2 mm KBr cells) and ^{1}H and ^{31}P NMR spectra.

X-ray Analysis of $[\{Fe(CO)_2[P(OEt)_3]_2\}_2\{\mu\text{-}4,4'\text{-}N_2(2\text{-}CH_3)C_6H_3{-}C_6H_3(2\text{-}CH_3)N_2\}](BPh_4)_2$ (5b). Suitable crystals for X-ray analysis were obtained by recrystallization from ethanol. Automatic peak search and indexing procedures carried out on a Siemens AED diffractometer yielded a triclinic primitive cell. Inspection of *E* statistics indicated the space group as $P\bar{1}$. Data on structure determination are summarized in Table 2. Unit-cell dimensions and their standard deviations were determined and refined from the angular positions of 25 carefully measured reflections. During data collection, the intensity of one standard reflection was monitored to check crystal decomposition or loss of alignment. No intensity decay was detected. Polarization and Lorentz effects were considered for data reduction. Both direct methods and the automatic Patterson procedure failed to identify the correct solution, and the best phase sets found in both cases presented four heavy collinear peaks spaced by approximately 2.2 Å in the *E*-map. When these apparent heavy atoms were used to phase the structure, a sort of dimeric molecule, consisting of the splitting and shift of the expected structure, appeared but did not refine. The correct position of the single Fe atom was finally located in the midpoint of the four heavy atom substructure when merging of the two images was observed. The two apparent heavy atoms in the initial solution were in fact at the midpoints of the collinear Fe−P bonds in the complex. The phasing power of the correctly placed Fe atom was sufficient to retrieve the entire structure by inspection of the Fourier electron density map.

The structure consists of discrete $[\{Fe(CO)_2[P(OEt)_3]_2\}_2\{\mu\text{-}4,4'\text{-}N_2\text{-}(2\text{-}CH_3)C_6H_3{-}C_6H_3(2\text{-}CH_3)N_2\}]^{2+}$ cations and BPh_4^- anions. All non-hydrogen atoms were initially refined by several cycles of full-matrix least-squares using F^2 by SHELXL96,[35] with isotropic thermal displacement parameters. At convergence, an empirical absorption correction was applied on F^2, following the method of Walker and Stuart.[36] This procedure produced a statistically significant *R*-factor drop, according to Hamilton's criteria.[37] Anisotropic thermal displacement parameters were then refined for all non-H atoms, and hydrogen atoms were placed at calculated positions, riding on their carrier atoms. The critical low ratio of "observed" to "measured" reflections prompted us to increase the number of observations and reduce the number of parameters with restraints and constraints in the refinement. Rigid-bond restraints were applied to the thermal motion of terminal ethyl groups and to the whole BPh_4^- anion, to prevent physically unreasonable modeling of these potentially disordered or mobile groups. In the latter, phenyl groups were also constrained to rigid-body behavior in order to decrease the number of refined parameters. The final difference density map was essentially featureless. Neutral scattering factors were employed and anomalous dispersion terms were included for non-hydrogen atoms. Calculations were performed on an ENCORE91 computer. The programs PARST95[38] and ZORTEP[39] were employed to analyze the final geometry. Use was made of the Cambridge Structural Database[40] facilities at the "Centro di Studio per la Strutturistica Diffrattometrica del C.N.R." in Parma. The complete list of atomic coordinates, geometric parameters, and thermal displacement parameters have been deposited in CIF format as Supporting Information.

Electrochemical Apparatus and Procedures. Voltammetric and chronoamperometric experiments were carried out in a three-electrode cell. The working electrode was a glassy carbon disk (diameter 0.5 cm) mirror-polished with graded alumina powder and surrounded by a platinum spiral counter electrode. The potential of the working electrode was probed by a Luggin capillary reference electrode compartment. All potentials were measured and refer to an aqueous KCl saturated Ag/AgCl reference electrode. The $E_{1/2}$ value for the ferrocene/ferricinium (Fc/Fc^+) couple measured in the supporting electrolyte used in this work was +520 mV vs Ag/AgCl. The specific resistance of the electrolyte solution, measured with a Crison CM 2202 conductometer, was 1250 Ω cm. All measurements were carried out at room temperature in a nitrogen atmosphere. The voltammetric equipment used was an Amel model 552 potentiostat, with positive feedback correction of uncompensated resistance, in conjunction with an Amel model 568 digital logic function generator, a Yokogawa 3023 *X*−*Y* recorder, or an EG&G-PAR model 273 potentiostat controlled by a personal computer via M270 software.

Digital simulations of the experimental voltammograms were carried out using Digisim 2.0 (BAS Inc.), a cyclic voltammetric simulation program, running on a HP 735/90 CPU Pentium computer. The voltammograms of the binuclear compounds were simulated by the following mechanism (Chart 2), where **A** is the starting binuclear compound.

For instance, in the case of $[\{Fe(CO)_2[P(OEt)_3]_2\}_2\{\mu\text{-}4,4'\text{-}N_2C_6H_4{-}C_6H_4N_2\}](BPh_4)_2$ (**5a**), the fit between simulated and experimental data was optimized by the following values of the simulation parameters:

$$E°(1) = 0.585\ \text{V}, \quad \alpha(1) = 0.1; \quad k_s(1) = 1 \times 10^{-5}\ \text{cm/s}$$

$$E°(2) = 0.615\ \text{V}, \quad \alpha(2) = 0.1; \quad k_s(2) = 5 \times 10^{-6}\ \text{cm/s}$$

$$E°(3) = -0.590\ \text{V}, \quad \alpha(3) = 0.9; \quad k_s(3) = 1.2 \times 10^{-5}\ \text{cm/s}$$

$$E°(4) = -0.550\ \text{V}, \quad \alpha(4) = 0.7; \quad k_s(4) = 5 \times 10^{-6}\ \text{cm/s}$$

$$K_{eq}(5) = 1 \times 10^9; \quad k_f(5) = 0.3\ \text{s}^{-1}$$

$$E°(6) = -0.685\ \text{V}, \quad \alpha(6) = 0.77; \quad k_s(6) = 1.15 \times 10^{-6}\ \text{cm/s}$$

$$D_A = D_B = D_C = D_D = D_E = D_F = 1.7 \times 10^{-5}\ \text{cm}^2\text{/s}$$

The voltammograms of the mononuclear compounds were simulated by a similar mechanism from which reactions 2 and 4 were excluded and reaction 5 became S = F.

Although positive feedback correction of the ohmic drop of the solution was used to obtain the experimental data, a good fit between the experimental and simulated voltammograms was achieved only by introducing in the simulations a residual uncompensated resistance of 700 Ω. The reliability of this value was confirmed by comparison

(35) Sheldrick, G. *SHELXL96. Program for structure refinement*, *β*-test version; University of Goettingen: Germany, 1996.
(36) Walker, N.; Stuart, D. *Acta Crystallogr.* **1983**, *A39*, 158.
(37) Hamilton, W. C. *Statistics in physical science*; The Ronald Press Company: New York, 1964.
(38) Nardelli, M. *J. Appl. Crystallogr.* **1995**, *28*, 659.
(39) Zsolnai, L.; Pritzkow, H. *ZORTEP. ORTEP original program modified for PC*; University of Heidelberg: Germany, 1994.
(40) Allen, F. H.; Kennard, O. *Chemical Design Automation News* **1993**, *8*, 1, and 31.

Chart 2

(oxidation) $B + e^- = A$ (1)

$C + e^- = B$ (2)

(reduction) $A + e^- = S$ (3)

$S + e^- = E$ (4)

$E = F$ (5)

$F + e^- = G$ (6)

between experimental and simulated cyclic voltammograms obtained at different scan rates in 2.5 mM solutions of ferrocene.

Results and Discussion

Hydride complexes $FeH_2(CO)_2P_2$ quickly react both with mono- (ArN_2^+) and bis-aryldiazonium ($^+N_2Ar-ArN_2^+$) cations to give the aryldiazenido derivatives $[Fe(ArN_2)(CO)_2P_2]^+$ (**1**−**4**) and $[\{Fe(CO)_2P_2\}_2(\mu\text{-}N_2Ar-ArN_2)](BPh_4)_2$ (**5**−**8**), respectively, which were isolated as BPh_4^- salts and characterized (Scheme 1).

When the reaction was carried out changing the solvent, temperature, and the ratio between the hydride and the diazonium salt, the aryldiazenido compound was always exclusively the product but was obtained in varying yields. The formation of an aryldiazenido compound from the reaction of a dihydride species of Fe(II) with aryldiazonium cation was surprising on the basis of previous results[1−5] and prompted us to investigate the reaction in detail. Results indicated the reaction path reported in Scheme 2, involving the formation of hydride−diazene intermediate **D**, which, through the loss of H_2, affords final aryldiazenido complexes **1**−**8**.

Scheme 1[a]

$$FeH_2(CO)_2P_2 \xrightarrow[CH_2Cl_2]{ArN_2^+,\ exc.} [Fe(ArN_2)(CO)_2P_2]^+ \quad \mathbf{1–4}$$

$$FeH_2(CO)_2P_2 \xrightarrow[(CH_3)_2CO]{^+N_2Ar–ArN_2^+,\ exc.} [\{Fe(CO)_2P_2\}_2(\mu\text{-}N_2Ar–ArN_2)]^{2+} \quad \mathbf{5–8}$$

[a] P = $P(OEt)_3$ (**1**, **5**), $PPh(OEt)_2$ (**2**, **6**), PPh_2OEt (**3**, **7**), $P(OPh)_3$ (**4**, **8**); Ar = C_6H_5 (**a**), 2-$CH_3C_6H_4$ (**b**), 4-$CH_3C_6H_4$ (**c**); Ar−Ar = 4,4′-$C_6H_4-C_6H_4$ (**a**), 4,4′-(2-CH_3)$C_6H_3-C_6H_3$(2-CH_3) (**b**), 4,4′-$C_6H_4-CH_2-C_6H_4$ (**d**).

Scheme 2

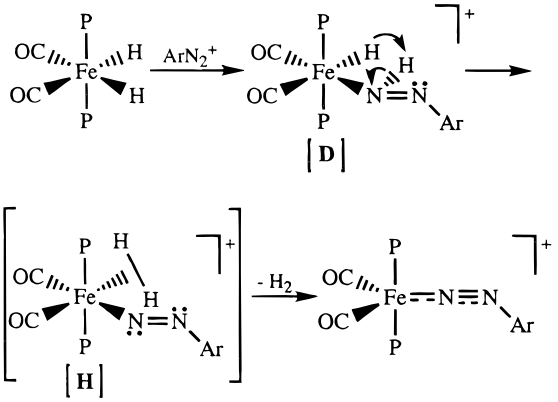

When the progress of the reaction between $FeH_2(CO)_2[P(OPh)_3]_2$ and 4-$CH_3C_6H_4N_2^+BF_4^-$ in $(CD_3)_2CO$ is followed by NMR spectroscopy, the initial appearance of a quite broad signal at 11.57 ppm in the ^1H spectra may be observed. This is split into a doublet ($^1J_{^{15}NH}$ = 65 Hz) using the labeled 4-$CH_3C_6H_4N{\equiv}{}^{15}N^+BF_4^-$ salt and strongly suggests the formation of an aryldiazene intermediate. Although such a diazene cannot be isolated, its formulation as a hydride−diazene complex (**D**) is supported by the appearance of a new hydride signal at −6.80 ppm (triplet) in the proton NMR spectra, besides the resonance of the starting $FeH_2(CO)_2P_2$ species at −11.18 ppm. A new singlet at 182.1 ppm in the ^{31}P spectrum is also observed. On these bases, it is reasonable to suppose that the reaction between $FeH_2(CO)_2P_2$ and ArN_2^+ proceeds with the initial insertion of the ArN_2^+ group into the FeH bond, giving the $[FeH(ArN{=}NH)(CO)_2P_2]^+$ (**D**) cation. As the reaction proceeds, the ^1H and ^{31}P spectra of the reaction mixture do not show the formation of other iron complexes in detectable amounts, except for the final aryldiazenido $[Fe(ArN_2)(CO)_2P_2]^+$ derivative. However, in the proton spectra, parallel with the appearance of the signals of the $[Fe(ArN_2)(CO)_2P_2]^+$ cation, there is also a small signal near 4.6 ppm, which decreases on shaking the NMR tube and may be attributed[41] to the signal of free H_2. The presence of molecular hydrogen in the reaction mixture may be explained by taking into account the known properties of both diazene and hydride ligands in iron(II) complexes,[1−5,42] i.e., the acidity of the diazene hydrogen atom on one hand and the easy protonation of the hydride ligand on the other, which potentially allow the formation of an η^2-H_2 ligand. Thus, an intramolecular acid−base reaction between the diazene proton of ArN═NH and the Fe−H hydride may give rise to a very unstable dihydrogen intermediate (**H**), which, by loss of H_2 and rearrangement of the ArN_2^- ligand to ArN_2^+ (see below), affords the final pentacoordinate iron(0) $[Fe(ArN_2)(CO)_2P_2]^+$ cation, in agreement with the proposed mechanism.

A comparison of these results with those previously reported by us[1−5,43] on the reactivity of iron(II) hydride of the type FeH_2P_4 and $[FeH(CO)P_4]^+$ with aryldiazonium cations shows that the formation, in the present case, of an aryldiazenido compound is plausible but at the same time somewhat surprising. The reaction of the dihydride species FeH_2P_4 with ArN_2^+ was reported[1] to give first the monoaryldiazene $[FeH(ArN{=}NH)P_4]^+$ complex, which further reacts with ArN_2^+ to give the bis(aryldiazene) $[Fe(ArN{=}NH)_2P_4]^{2+}$ derivative. Treatment of the bis(aryldiazene) with base gives the $[Fe(ArN_2)P_4]^+$ aryldiazenido compound through deprotonation of one ArN═NH ligand and concurrent dissociation of the other. The hydride−monoaryldiazene $[FeH(ArN{=}NH)P_4]^+$ derivative, instead, is practically unreactive toward bases in every set of conditions. However, the formation of an aryldiazenido complex from a monoaryldiazene complex of iron(II) has been observed[42] to take place only in complexes of the type $[Fe(ArN{=}NH)(RCN)P_4]^{2+}$, containing the rather labile RCN ligand, the easy dissociation of which allows the following reaction (Scheme 3) to take place. The presence of two strong π-acceptor CO ligands in our $[FeH(ArN{=}NH)(CO)_2P_2]^+$ (**D**) monoaryldiazene intermediate probably makes the diazene hydrogen atom so acidic that an intramolecular acid−base reaction with the hydride ligand affords H_2 and the $[Fe(ArN_2)(CO)_2P_2]^+$ aryldiazenido derivative.

(41) Crabtree, R. H.; Lavin, M.; Bonneviot, L. *J. Am. Chem. Soc.* **1986**, *108*, 4032.

(42) Albertin, G.; Antoniutti, S.; Bordignon, E. *J. Am. Chem. Soc.* **1989**, *111*, 2072.

Scheme 3[a]

$$[Fe(ArN{=}NH)(RCN)P_4]^{2+} + NEt_3 \longrightarrow [Fe(ArN_2)P_4]^{+} + NHEt_3^{+} + RCN$$

[a] R = 4-$CH_3C_6H_4$; P = $P(OEt)_3$.

Chart 3

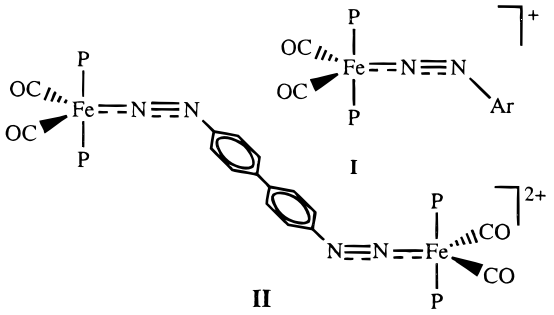

Both mono- (**1**−**4**) and binuclear (**5**−**8**) aryldiazenido complexes are red or orange solids stable in air and in solutions of polar organic solvents, where they behave as 1:1 or 2:1 electrolytes.[44] Elemental analyses and spectroscopic properties (Table 1) confirm the proposed formulation. The IR spectra show two ν(CO) bands at 2056−1972 cm^{-1}, in agreement with two carbonyl ligands in a mutually cis position. The ν(NN) band of the aryldiazenido ligand is also present in the 1779−1720 cm^{-1} region and is shifted to lower frequencies (about 35 cm^{-1}) in the labeled ArN≡^{15}N compound, according to the proposed assignment. These values for the N−N stretching frequency are indicative[45] of a singly bent aryldiazenido ligand, and this statement was shown to be correct by X-ray structure determination of **5b**, discussed below. The ^{15}N NMR spectra also fit the presence of a singly bent ArN_2 ligand,[46,47] showing a triplet at 19.7 ppm ($^2J_{^{15}N^{31}P}$ = 20 Hz) due to coupling with two magnetically equivalent phosphorus nuclei for the [Fe($C_6H_5N{\equiv}^{15}N$)$(CO)_2${$P(OEt)_3$}$_2$]BPh_4 (**1a$_1$**) derivative.

In the temperature range between +30 and −90 °C, the ^{31}P-{^{1}H} NMR spectra appear as a sharp singlet, suggesting the presence of two magnetically equivalent phosphine ligands. Furthermore, a complicated multiplet is present in the methylene proton region of the ^{1}H NMR spectra, suggesting the presence of two phosphites in a mutually trans position. On these bases, a trigonal bipyramidal geometry of the type shown in **I** and **II** (Chart 3) and similar to that determined in the solid state for **5b** (Figure 1) can be proposed in solution for both mono- (**1**−**4**) and binuclear (**5**−**8**) aryldiazenido compounds.

A comparison of the spectroscopic properties of ArN_2 complexes **1**−**8** shows, first of all, that there is practically no difference between mono- and binuclear complexes containing the same phosphite ligand. Instead, variation of the $\nu(N_2)$ frequency on changing the π-acceptor properties of the phosphite ligand was observed in all compounds, with the highest $\nu(N_2)$ value of 1779 cm^{-1} being observed in the [Fe(2-$CH_3C_6H_4N_2$)-$(CO)_2${$P(OPh)_3$}$_2$]BPh_4 complex, containing the larger[48,49] π-acceptor phosphite ligand.

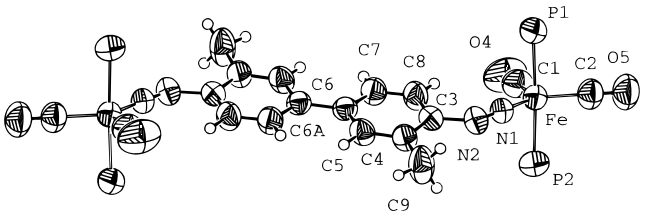

Figure 1. ORTEP view of dimeric cation [{$Fe(CO)_2$[$P(OEt)_3$]$_2$}$_2${μ-4,4′-N_2(2-CH_3)C_6H_3−C_6H_3(2-CH_3)N_2}]$^{2+}$ (**5b**) with 50% probability thermal ellipsoids. Ethoxy groups have been omitted for clarity. Molecule is centrosymmetric around midpoint of bond C6−C6A.

Scheme 4[a]

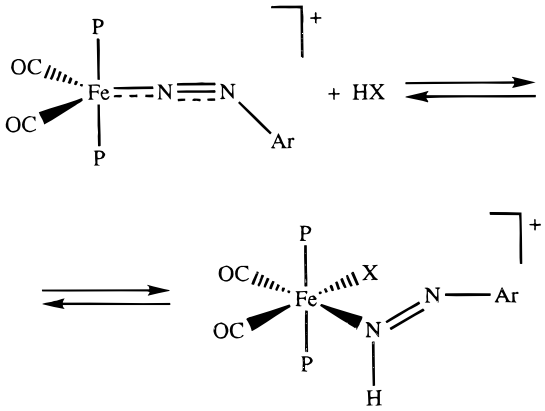

[a] HX = CF_3SO_3H, CF_3COOH, HCl.

Aryldiazenido complexes **1**−**8** react with an excess of strong acid containing a good coordinating anion such as CF_3SO_3H, CF_3COOH, or HCl to give a yellow solution whose IR and NMR spectra indicate the presence of an aryldiazene complex, as shown in Scheme 4. The addition of HX to **1a**, **1c**, or **5b** does cause the appearance of a diazene proton signal (a doublet using the labeled ArN≡^{15}N compound) near 13.0 ppm in the ^{1}H NMR spectra, while a new singlet, in addition to the signal of the starting [$Fe(ArN_2)(CO)_2P_2$]$^+$ cation, appears in the ^{31}P spectra. The ^{15}N NMR spectra of the [FeCl($C_6H_5N{=}^{15}NH$)-$(CO)_2${$P(OEt)_3$}$_2$]$^+$ cation was also detected and showed the signal at −2.7 ppm (in CD_2Cl_2 at −80 °C) with a $^2J_{^{15}N^{31}P}$ of about 12 Hz. The disappearance of the $\nu(N_2)$ absorption is also observed in the IR spectra, together with the appearance of two new ν(CO) bands due to the diazene complex. However, spectroscopic studies on the reaction course show that a large excess of acid HX must be added to the aryldiazenido complex in order to obtain the corresponding aryldiazene and that the removal of HX gives back the [$Fe(ArN_2)(CO)_2P_2$]$^+$ derivative. The equilibrium of the reaction of Scheme 4 also prevents aryldiazene derivatives from being obtained in pure form, as the aryldiazenido complex is the predominant species in the resulting solid.

Apart from reactions with acid, aryldiazenido **1**−**8** are very robust complexes, which are inert to substitution by several ligands such as CO, phosphites, ArN_2^+, and halogenide ions, as well as to oxidation with Br_2 or I_2. Only with *p*-tolyl isocyanide was the slow substitution of the carbonyl ligand observed, although the result was intractable oils, which were not characterized.

X-ray Crystal Structure of [{$Fe(CO)_2$[$P(OEt)_3$]$_2$}$_2${μ-4,4′-N_2(2-CH_3)C_6H_3−C_6H_3(2-CH_3)N_2}]$(BPh_4)_2$ (5b). The cation consists of a binuclear complex in which the 4,4′-N_2(2-CH_3)-

(43) Albertin, G.; Antoniutti, S.; Lanfranchi, M.; Pelizzi, G.; Bordignon, E. *Inorg. Chem.* **1986**, *25*, 950.
(44) Geary, W. J. *Coord. Chem. Rev.* **1971**, *7*, 81.
(45) Haymore, B. L.; Ibers, J. A. *Inorg. Chem.* **1975**, *14*, 3060.
(46) Haymore, B. L.; Hughes, M.; Mason, J.; Richards, R. L. *J. Chem. Soc., Dalton Trans.* **1988**, 2935.
(47) Dilworth, J. R.; Kan, C. T.; Richards, R. L.; Mason, J.; Stenhouse, I. *J. Organomet. Chem.* **1980**, *201*, C24.
(48) Tolman, C. A. *Chem. Rev.* **1977**, *77*, 313.
(49) Rahman, M. M.; Liu, H.-Y.; Eriks, K.; Prock, A.; Giering, W. P. *Organometallics* **1989**, *8*, 1.

Table 3. Most Relevant Bond Distances (Å) and Angles (deg) with Uncertainties in Parentheses (C6A at $-x + 1, -y, -z + 1$) for Compound **5b**

		Distances	
Fe−P1	2.223(3)	C3−C4	1.381(9)
Fe−P2	2.208(3)	C3−C8	1.368(9)
Fe−N1	1.702(5)	C4−C5	1.376(8)
Fe−C1	1.758(7)	C4−C9	1.500(10)
Fe−C2	1.786(6)	C5−C6	1.385(9)
O4 −C1	1.144(10)	C6−C7	1.398(8)
O5−C2	1.143(8)	C7−C8	1.351(8)
N1−N2	1.189(7)	C6−C6A	1.499(7)
N2−C3	1.451(7)		
		Angles	
C1−Fe−C2	101.1(3)	Fe−C2−O5	179.9(6)
N1−Fe−C2	136.3(3)	N2−C3−C8	120.4(5)
N1−Fe−C1	122.6(3)	N2−C3−C4	117.4(5)
P2−Fe−C2	91.6(3)	C4−C3−C8	122.1(6)
P2−Fe−C1	88.8(3)	C3−C4−C9	122.1(5)
P2−Fe−N1	88.0(2)	C3−C4−C5	116.2(5)
P1−Fe−C2	90.5(3)	C5−C4−C9	121.8(6)
P1−Fe−C1	90.2(3)	C4−C5−C6	124.0(6)
P1−Fe−N1	90.9(2)	C5−C6−C7	116.4(5)
P1−Fe−P2	177.8(1)	C6−C7−C8	121.2(6)
Fe−N1−N2	174.8(5)	C3−C8−C7	120.1(6)
N1−N2−C3	123.6(5)	C5−C6−C6A	121.8(5)
Fe−C1−O4	178.9(7)	C7−C6−C6A	121.8(5)

$C_6H_3-C_6H_3(2\text{-}CH_3)N_2$ ligand bridges two Fe atoms by means of the two terminal diazo groups. Figure 1 shows the molecular structure of the cation, together with the labeling scheme. Table 3 lists the most important geometric parameters of the cation. The two iron atoms are 13.87 Å apart. The molecule lies on a crystallographic center of symmetry, located at the midpoint of the C6−C6A bond. The metal binds one nitrogen belonging to the 4,4′-$N_2(2\text{-}CH_3)C_6H_3-C_6H_3(2\text{-}CH_3)N_2$ ligand, two carbonyls, and two $P(OEt)_3$ groups. The coordination polyhedron is a quite regular trigonal bipyramid, with the two phosphites at the apical positions, and the P−O vectors are staggered with respect to the equatorial C−O groups. The greatest distortion from ideal geometry is in the equatorial plane, where the angle N1−Fe−C2 becomes wider (136.3(3)°) at the expense of C1−Fe−C2, which narrows (101.1(3)°). This distortion is due to the short repulsive interaction O5···O5 ($-x, 1 - y, -z$) = 3.161(8) Å, which is the only significant contact found in the crystal packing of the compound. The bond geometry for the diazo group is linear at N1 (Fe−N1−N2 = 174.8(5)°) and trigonal at N2 (N1−N2−C3 = 123.6(5)°). The metal complex is located trans to the *o*-methyl group (C4−C3−N2−N1 = 167.9(6)°). Despite the slight rotation of the *o*-toluyl group around the C3−N2 bond, indicated by the torsion angle C8−C3−N2−N1 = −15(1)°, the entire ligand in the dimer is coplanar within 0.5 Å to the equatorial plane of the complex trigonal bipyramids.

This dimeric structure is similar to those of the pentacoordinated monomeric complexes $[Fe(CO)_2(PPh_3)_2(C_6H_5N_2)]BF_4$[50] and $[Fe(4\text{-}CH_3C_6H_4N_2)\{P(OEt)_3\}_4]BPh_4$.[1] The geometry of the Fe−N−N−C system is well preserved, and the average dimensions for the three compounds are Fe−N = 1.69(1), N−N = 1.20(1), and N−C = 1.44(2) Å. The bond geometry of carbonyl coordination is in agreement with that observed in $[Fe(CO)_2(PPh_3)_2(C_6H_5N_2)]BF_4$,[50] where narrowing of the C−Fe−C angle is also found (108°).

The crystal structure of a symmetric dimeric iron complex, $[\{FeH[P(OEt)_3]_4\}_2\{\mu\text{-}4,4'\text{-}HN{=}N(2\text{-}CH_3)C_6H_3-C_6H_3(2\text{-}CH_3)N{=}NH\}](BPh_4)_2$, is known,[5] in which the ligand is protonated on N1 at both ends and a hydride enters the metal coordination sphere, which expands to octahedral. For the protonated ligand, distances Fe−N1 and N1−N2 are much longer (1.913 and 1.273 Å, respectively) than those in the present case, while N2−C3 is not significantly affected (1.415 Å). The linear geometry for N1 is also lost (N2−N1−Fe = 132°), and the torsion angle C8−C3−N2−N1 = −37° shows that the rotation of the aromatic plane around the C3−N2 bond is more pronounced for the protonated ligand.

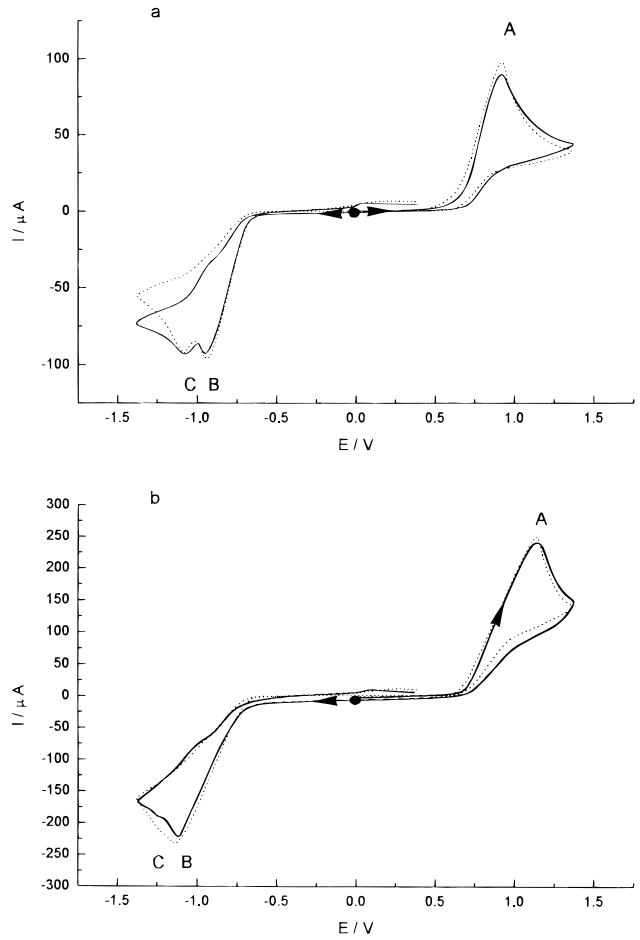

Figure 2. Experimental (full lines) and simulated (dotted lines) cyclic voltammograms obtained in 2.5 mM $[\{Fe(CO)_2[P(OEt)_3]_2\}_2\{\mu\text{-}4,4'\text{-}N_2C_6H_4-C_6H_4N_2\}]^{2+}$ (**5a**) at 20 mV/s (a) and 200 mV/s (b). Supporting electrolyte: 0.1 M tetrabutylammonium hexafluorophosphate (TBAH)/dichloroethane (DCE). Working electrode: glassy carbon. Direct oxidation scan: initial potential = 0.0 V; vertex potential = 1.4 V; final potential = 0.0 V. Direct reduction scan: initial potential = 0.0 V; vertex potential = −1.4 V; final potential = 0.4 V.

Electrochemical Studies. Figure 2a (full line) shows the cyclic voltammogram of 2.5 mM $[\{Fe(CO)_2[P(OEt)_3]_2\}_2\{\mu\text{-}4,4'\text{-}N_2C_6H_4-C_6H_4N_2\}](BPh_4)_2$ (**5a**) in 0.1 M TBAH/DCE, recorded at 20 mV/s. The dotted line shows the simulated voltammogram resulting from mechanisms 1−6 (Chart 2). The direct oxidation scan is characterized by an irreversible oxidation peak, A. In the direct reduction scan, two peaks are observed: one main peak, B, followed by a smaller peak, C. Relevant peak potential values are reported in Table 4. As shown in Figure 2b, these peak values change slightly when the scan rate is increased. The satisfactory fit with the simulated data indicates that such shifts are fully matched by mechanisms 1−6 (Chart 2), even if it is necessary to take into account also some residual ohmic drop resistance not fully compensated by the use of positive feedback (see Experimental Section).

Peaks A and B are irreversible when the scan rate is increased to 1 V/s (not shown in figure). The currents of peaks A and B

(50) Haymore, B. L.; Ibers, J. A. *Inorg. Chem.* **1975**, *14*, 1369.

Table 4. Selected Electrochemical Data for Iron Complexes

compd	$(E_{pred})_B$ (mV)[a]	$(I_{pred})_B/Cv^{1/2}$ [c]	n[b]	$(E_{pred})_C$ (mV)[a]	$(E_{pox})_A$ (mV)[a]	$(I_{pox})_A/Cv^{1/2}$ [c]	n[b]
1c $[Fe(4\text{-}CH_3C_6H_4N_2)(CO)_2\{P(OEt_3\}_2]^+$	−940	106	1	−1030	+860	113	1
5a $\{[Fe(CO)_2\{P(OEt)_3\}_2]_2(\mu\text{-}4,4'\text{-}N_2C_6H_4{-}C_6H_4N_2)\}^{2+}$	−950	156	2	−1090	+920	230	2
5b $\{[Fe(CO)_2\{P(OEt)_3\}_2]_2[\mu\text{-}4,4'\text{-}N_2(2\text{-}CH_3)C_6H_3{-}C_6H_3(2\text{-}CH_3)N_2]\}^{2+}$	−910	216	2	−1030	+930	260	2
6b $\{[Fe(CO)_2\{PPh(OEt)_2\}_2]_2[\mu\text{-}4,4'\text{-}N_2(2\text{-}CH_3)C_6H_3{-}C_6H_3(2\text{-}CH_3)N_2]\}^{2+}$	−1000	184	2	−1090	+890	230	2
5d $\{[Fe(CO)_2\{P(OEt)_3\}_2]_2(\mu\text{-}4,4'\text{-}N_2C_6H_4{-}CH_2{-}C_6H_4N_2)\}^{2+}$	−920	163	2	−1040	+920	235	2

[a] Voltammetric peak potential values measured at 20 mV/s in 0.1 M TBAH/DCE containing 2.5 mM of examined compound. [b] Calculated from ratio of slopes of I_c vs $t^{-1/2}$ plots obtained by chronoamperometric experiments carried out on equimolar solutions of ferrocene and the compound under study. [c] Peak currents normalized over solution concentration, C (mM), of the compound and square root of scan rate (slope of I_p (μA) vs $v^{1/2}$ ($V^{1/2}$ $s^{-1/2}$) linear plots).

increase linearly with the square root of the scan rate, indicating diffusive control for the processes at both peaks.

The peak current of peak A is roughly equal to the current of peak B and is about 1.7 times higher than the oxidation peak current recorded on a 2.5 mM ferrocene solution in the same electrolyte. It is well-known[51,52] that ferrocene undergoes a one-electron reversible oxidation process; however, since the electrochemical processes under study are irreversible, no final information on the number of electrons exchanged in the electrode reaction can be obtained by the simple comparison of voltammetric peak currents. To this aim, it is more appropriate to compare the slope of chronoamperometric current, I_c, with the reciprocal of the square root of time. This slope is in fact directly proportional to the number of electrons exchanged, n, independently of the reversibility degree of the process.[53] Assuming that the ratio between the square roots of the diffusion coefficients of **5a** and ferrocene is 1, comparison of the slopes of I_c vs $t^{-1/2}$ plots for the two compounds gives a value of $n = 2$, both for oxidation at peak A and reduction at peak B of **5a**. The voltammogram shown in Figure 2b indicates that the current of peak C decreases progressively as the scan rate is increased, showing that peak C has a kinetic character. Similar patterns and peak potential values are also obtained for all binuclear compounds **5b**, **5d**, and **6b** containing $P(OEt)_3$ or $PPh(OEt)_2$ as ligands; the relevant electrochemical data are listed in Table 4.

Figure 3 shows cyclic voltammograms recorded on a 2.8 mM solution of the parent mononuclear compound $[Fe(4\text{-}CH_3C_6H_4N_2)(CO)_2\{P(OEt)_3\}_2]BPh_4$ (**1c**). Now, the currents of peaks A and B (normalized with respect to the concentration) are about half of those recorded for $[\{Fe(CO)_2[P(OEt)_3]_2\}_2\{\mu\text{-}4,4'\text{-}N_2C_6H_4{-}C_6H_4N_2\}](BPh_4)_2$ (**5a**) and the other binuclear compounds. Interestingly, the shapes of the voltammograms, in particular the difference between the peak and half-peak potentials of **1c** and **5a**, remain unchanged.

All the above experimental evidence indicates that, for the binuclear compounds studied here, although both reduction and oxidation are electron-transfer processes involving two electrons, they are really composed of two separate one-electron processes. The observed voltammetric behavior is typical of molecules containing two localized redox centers.[54] For reversible processes, it was shown that, when the difference in formal potential $\Delta E^\circ = 35.6$ mV,[55,56] the two centers do not interact. In these conditions, the peak parameters are the same as those of a one-electron-transfer process, the only difference being an increase in peak current. The satisfactory fit between simulated and experimental data indicates that this situation also applies to the processes under study, even if they are irreversible.

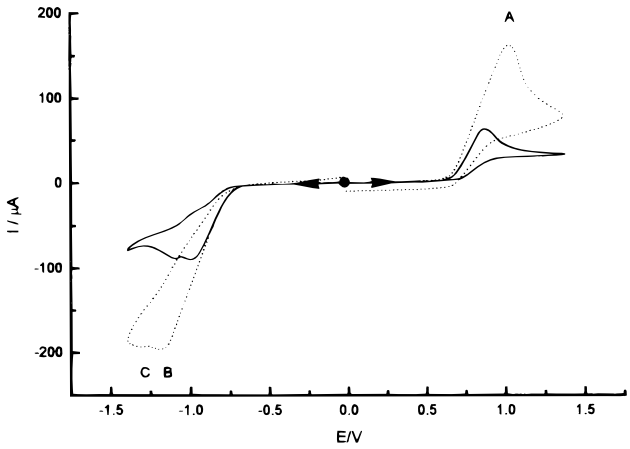

Figure 3. Cyclic voltammograms obtained in 2.8 mM $[Fe(4\text{-}CH_3C_6H_4N_2)(CO)_2\{P(OEt)_3\}_2]^+$ (**1c**) at 20 mV/s (full line) and 200 mV/s (broken line). Other experimental conditions are as in Figure 2. Direct oxidation scan: initial potential = 0.0 V; vertex potential = 1.4 V; final potential = 0.0 V. Direct reduction scan: initial potential = 0.0 V; vertex potential = −1.4 V; final potential = 0.0 V.

The scheme of the reactions that take place at the electrode/solution interface may be represented as follows:

$$[Fe{-}Fe]^{2+} \rightarrow [Fe{-}Fe]^{3+} + e^- \quad (7)$$

$$[Fe{-}Fe]^{3+} \rightarrow [Fe{-}Fe]^{4+} + e^- \quad (8)$$

$$[Fe{-}Fe]^{2+} + e^- \rightarrow [Fe{-}Fe]^{+} \quad (9)$$

$$[Fe{-}Fe]^{+} + e^- \rightarrow [Fe{-}Fe]^{0} \quad (10)$$

where $[Fe{-}Fe]^{2+}$ indicates a generic binuclear complex **5a**, **5b**, **5d**, or **6b**.

Since $E^\circ(8)$ is only a few tens of a millivolt more positive than $E^\circ(7)$ (see $E^\circ(1)$ and $E^\circ(2)$ in the simulations), only one oxidation peak A is observed; the same, with opposite signs, holds for reactions 9 and 10 and peak B.

The zero-charged reduction product is unstable and reacts to give the unknown product P

$$[Fe{-}Fe]^{0} \rightarrow P \quad (11)$$

which is reduced at peak C to generate the unknown reduced product Q.

$$P + e^- \rightarrow Q \quad (12)$$

(51) Kadish, K. M.; Ding, J. Q.; Malinski, T. *Anal. Chem.* **1984**, *56*, 1741.
(52) Bond, A. M.; Henderson, T. L. E.; Mann, D. R.; Mann, T. F.; Thorman, W.; Zoski, C. G. *Anal. Chem.* **1988**, *60*, 1878.
(53) Bard, A. J.; Faulkner, L. R. *Electrochemical Methods*; Wiley: New York, 1980.
(54) Bott, A. W. *Curr. Sep.* **1997**, *16*, 61.
(55) Flanagan, J. B.; Margel, S.; Bard, A. J.; Anson, F. C. *J. Am. Chem. Soc.* **1978**, *100*, 4248.
(56) Ammar, F.; Saveant, J. M. *J. Electroanal. Chem.* **1973**, *47*, 115.

In the case of mononuclear compound **1c**, both oxidation and reduction are one-electron irreversible processes.

$$[Fe]^{+} \rightarrow [Fe]^{2+} + e^{-}(\text{peak A}) \quad (13)$$

$$[Fe]^{+} + e^{-} \rightarrow [Fe]^{0}(\text{peak B}) \quad (14)$$

where $[Fe]^{+}$ indicates mononuclear complex **1c**.

Reaction 14 is followed by a chemical and electrochemical reaction equivalent to reactions 11 and 12 shown for the binuclear compounds. This evidence, together with the observation that peak potentials are almost the same for all the examined compounds (both mono- and binuclear), suggests that each iron center exchanges one electron, behaving independently of the oxidation state of the other metal center. Similar behavior has been observed for some bridged biferrocenes;[57] when the bridge was $-C(CH_3)_2-C(CH_3)_2-$, $-Hg-$, or $-CH=CH-C_6H_4-CH=CH-$, the two iron centers did not interact and the biferrocenes exhibited one irreversible two-electron oxidation wave.

Chart 4[a]

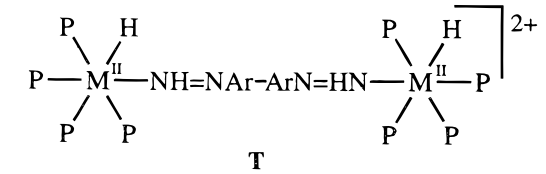

T

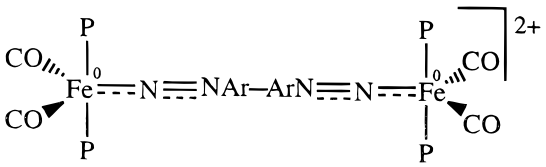

Z

[a] M = Ru, Fe; Ar−Ar = 4,4′-$C_6H_4-C_6H_4$, 4,4′-(2-CH_3)$C_6H_3-C_6H_3$(2-CH_3), 4,4′-$C_6H_4-CH_2-C_6H_4$.

A comparison of the electrochemical results of bis(aryldiazenido) iron compounds **5** and **6** (**Z**, Chart 4) with those previously obtained by us[5] on iron and ruthenium binuclear complexes of the type $[\{MHP_4\}_2(\mu\text{-HN=NArArN=NH})](BPh_4)_2$ (**T**, Chart 4), containing a bis(aryldiazene) as the bridging unit, shows the unexpectedly different behavior of the two classes of compounds. When conjugation between the metal centers is possible, the reduction of binuclear bis(aryldiazene) **T** proceeds via two separated one-electron reduction steps, which take place at well-separated potential values; when only the conjugation is hindered (as with the HN=$NC_6H_4-CH_2-C_6H_4N$=NH ligand), the difference in potential for the two consecutive reductions decreases dramatically and the two electrons are exchanged roughly at the same potential value. On the contrary, for all the bis(diazenido) iron compounds **Z**, the reduction proceeds via two independent one-electron processes, which give rise to only one voltammetric peak.

The electrochemical behavior of our binuclear compounds **5** and **6** is similar to that observed for the reduction of $[\{MHP_4\}_2(\mu\text{-HN=NC}_6\text{H}_4\text{-CH}_2\text{-C}_6\text{H}_4\text{N=NH})]^{2+}$ cations, in which conjugation between the two metal centers is hindered and the lack of any interaction always appears to be operative, even when the possibility of conjugation between the two iron centers is not interrupted by the introduction of interposed saturated functional groups, as in **5d**. This different electrochemical behavior for the binuclear complexes of types **T** and **Z** may be attributed to the differences in the oxidation number (two for **T** and zero for **Z**), geometry, and electronic configuration of the metal center, as well as to the properties of the bridging ligand, which may behave as an insulator in bis(aryldiazenido) iron derivatives. However, other binuclear complexes with both bis(aryldiazenido) and bis(aryldiazene) as bridging ligand must be prepared and their properties studied for better understanding of the properties of these new classes of derivatives.

Conclusions

Binuclear complexes with bis(aryldiazenido) bridging units of the type $[\{Fe(CO)_2P_2\}_2\{\mu\text{-4,4′-N}_2\text{Ar−ArN}_2\}](BPh_4)_2$ (**5**−**8**) may easily be prepared by reacting dihydride species $FeH_2(CO)_2P_2$ with the bis(aryldiazonium) cations $(N_2Ar-ArN_2\})(BF_4)_2$. The related mononuclear complexes $[Fe(ArN_2)(CO)_2P_2]BPh_4$ were also prepared, and the first structural parameters for binuclear bis(aryldiazenido) complexes are reported. Among the properties shown by these complexes is the electrochemical behavior, which shows that both iron centers can be oxidized or reduced via one-electron processes for each iron, with standard potentials roughly equal for both centers. Furthermore, aryldiazene $[FeX(ArN=NH)(CO)_2P_2]^{+}$ cations can be obtained in solution by a protonation reaction with strong acids of aryldiazenido derivatives **1**−**8**.

Acknowledgment. The financial support of MURST and the CNR, Rome, is gratefully acknowledged. We thank Dr. G. Balacco (Menarini Ricerche S.p.A.) for the license of use of his NMR software SwaN-MR. We thank D. Baldan for technical assistance.

Supporting Information Available: One X-ray crystallographic file, in CIF format, is available on the Internet only. Access information is given on any current masthead page.

IC980430E

(57) Morrison, W. H.; Krogsrud, S.; Hendrickson, D. N. *Inorg. Chem.* **1973**, *12*, 1998.